Hydrogels Based on Poly(ethylene oxide) and Poly(tetramethylene oxide) or Poly(dimethyl siloxane). II. Physical Properties and Bacterial Adhesion

Jae Hyung Park, You Han Bae

Center for Biomaterials and Biotechnology, Department of Materials Science and Engineering, Kwangju Institute of Science and Technology, 1 Oryong-dong, Puk-gu, Kwangju 500-712, South Korea

Received 25 January 2002; 23 October 2002

ABSTRACT: To investigate the effects of polymer chemistry and topology on physical properties and bacterial adhesion, various hydrogels composed of short hydrophilic [poly(ethylene oxide) (PEO)] and hydrophobic blocks were synthesized by polycondensation reactions. Differential scanning calorimetry and X-ray diffraction analysis confirmed that all of the hydrogels were strongly phase-separated due to incompatibility between PEO and hydrophobic blocks such as poly(tetramethylene oxide) (PTMO) and poly(dimethyl siloxane) (PDMS). The crystallization of PEO in the hydrogels was enhanced by the incorporation of longer PEO chains, the adoption of PDMS as a hydrophobic block, and the grafting of monomethoxy poly(ethylene oxide) (MPEO). Compared to Pellethane, the control polymer, the hydrogels exhibited higher Young's moduli and elongations at break, which was attributed to the crystalline domains of PEO and the flexible characteristics of the hydrophobic blocks. The mechanical properties of the hydrogels, however, significantly deteriorated when they were hydrated in distilled water; this was primarily ascribed to the disappearance of PEO crystallity. The water capacity of hydrogels at 37°C in phosphate-buffered saline (PBS) (pH = 7.4) was dominantly dependant on PEO content, which also influenced the thermonegative swelling behavior. From the bacterial adhesion tests, it was evident that both *S. epidermidis* and *E. coli* adhered to Pellethane much greater than to the hydrogels, regardless of the preadsorption of albumin. Better resistance to bacterial adhesion was observed in hydrogels with longer PEO chains, with PTMO as a hydrophobic block, and with MPEO grafts. The least bacterial adhesion for both species was achieved on $MPEO_{2k}$–PTMO, a hydrogel with MPEO grafts. © 2003 Wiley Periodicals, Inc. J Appl Polym Sci 89: 1505–1514, 2003

Key words: hydrogels; physical properties; biocompatibility; biomaterials

INTRODUCTION

With nontoxicity and biocompatibility, hydrogels, which swell in water and retain a significant amount of water within their structure, have been extensively investigated for biomedical applications, including contact lenses, catheters, wound dressings, and ureteral stents.[1] To assess the feasibility for their use as biomedical devices, the physical properties of a specific hydrogel should be considered for a desired application. To adjust the mechanical properties of chemically crosslinked hydrogels, approaches that have been considered include alteration or the comonomer composition, controlling of the crosslinking density, and a change in polymerization condition.[2] Meanwhile, the three-dimensional stability of thermoplastic hydrogels, which are physically crosslinked, is governed by physical junction domains associated with hydrogen bonding, hydrophobic interaction, crystallinity, and ionic complexation.[3–5]

One of the limiting factors for the extended use of surgical implants is biomaterial-centered infection, involving the initial adhesion of bacteria and subsequent colonization.[6] Once established on the polymeric surfaces, infections are extremely resistant to antibiotics and any host defense mechanism until the device is removed.[7,8] Initial bacterial adhesion, a critical event in the phathogenesis of foreign-body infection, might be preceeded by many factors, including the characteristics of bacteria itself, the surface properties of biomaterial, and other environmental factors, such as the presence of serum proteins or antibiotics.[9] Although the role of bacterial adhesion and colonization on the biomaterial surface is not fully understood, researchers believe that the adhesion is relevant to physical interactions between bacteria and biomaterial surfaces and receptor-specific bindings.[6] Recent reports have suggested that hydrophobic interactions seem to be the most important factor.[10,11]

In a previous study, we developed a novel type of hydrogel based on poly(ethylene oxide) (PEO) and poly(tetramethylene oxide) (PTMO) or poly(dim-

Correspondence to: Y. H. Bae (you.bae@m.cc.utah.edu).

Contract grant sponsor: Ministry of Health and Welfare, Korea; contract grant number: HMP-98-G-2-034.

Journal of Applied Polymer Science, Vol. 89, 1505–1514 (2003)
© 2003 Wiley Periodicals, Inc.

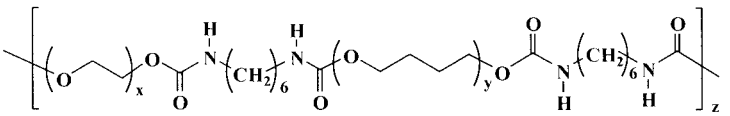

$PEO_{2k}PTMO$ or $PEO_{3.4k}PTMO$

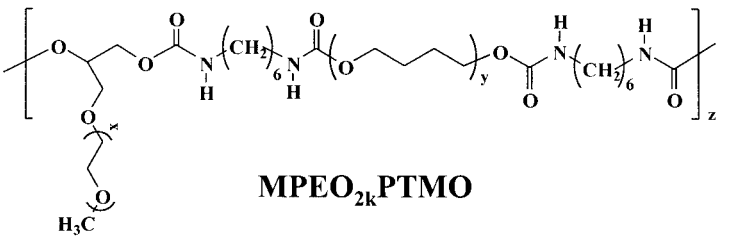

$MPEO_{2k}PTMO$

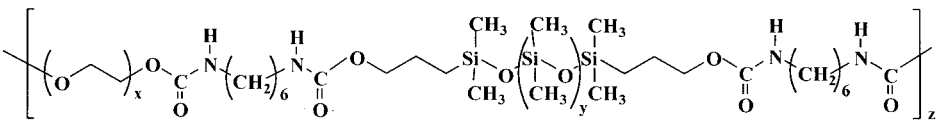

$PEO_{3.4k}PDMS$

Figure 1 Chemical structures of the hydrogels synthesized in this study.

ethyl siloxane) (PDMS).[12] The results demonstrated that the synthesized hydrogels exhibited a significantly lower adsorption of serum proteins and were much more resistant to platelet adhesion compared to Pellethane. Furthermore, their surface characteristics and composition of adsorbed proteins were dependant on the PEO block length, hydrophobic components, and polymer topology. Along this line of research, this study aimed to investigate the effects of polymer chemistry and topology on physical properties and bacterial adhesion, which may contribute to the development of biocompatible polymers for various applications. Pellethane, a commercially available polyurethane elastomer, was used as a control because it has received considerable attention as a candidate for biomedical applications. Physical properties were characterized with differential scanning calorimetry (DSC) X-ray diffraction; and tensile testing. The swelling kinetic and thermosensitive swelling behavior in PBS (pH = 7.4) were also examined. In addition, bacterial adhesion before and after serum albumin treatment was investigated by treatment with an inoculum containing microorganisms commonly implicated in biomaterial-centered infections, such as *Staphylococcus epidermidis (S. epidermidis)* and *Esherichia coli (E. coli).*

EXPERIMENTAL

Materials

PEO [PEO_{2k} and $PEO_{3.4k}$ for PEO with number-average molecular weights (M_n's) of 2000 and 3400 g mol^{-1}, respectively]; monomethoxy poly(ethylene oxide) (MPEO; M_n = 2000 g mol^{-1}), and PTMO (M_n = 2000 g mol^{-1}) were purchased from Aldrich (Milwaukee, WI) and were dried for 5 h at 80°C in a vacuum before use. α-ω-Dihydroxypropyl PDMS (M_n = 1860 g mol^{-1}; ShinEtsu, Tokyo, Japan) was treated with molecular sieves (4 Å, Aldrich) for 1 day and degassed for 5 h at 50°C in a vacuum before use. Pellethane 2363-80AE (Dow Chemical, Midland, MI), one of the representative polymeric biomaterials, was precipitated in methanol after being dissolved in dimethyl acetamide (J. T. Baker). It was then used as a control in most experiments after being dried for 2 days at 50°C in a vacuum. All solvents and chemicals relevant to the polymer synthesis were used after typical purification steps or with analytical grades. Bovine serum albumin (BSA) was purchased from Sigma (St. Louis, MO) and was used as received.

Synthesis

Detailed synthesis procedures are described in our previous report.[12] The chemical structures of the syn-

thesized hydrogels are presented in Figure 1. A brief description for the polymer syntheses follows:

MPEO terminated with propylene glycol

MPEO terminated with propylene glycol, containing two hydroxyl groups at one end, was synthesized in a two-step synthetic procedure. In the first step, MPEO glycidyl ether was prepared by the procedure described by Bergström et al.[13] In the second step, the MPEO glycidyl ether solution in distilled water was slowly added to 0.1*N* $HClO_4$ solution to generate propylene glycol in the chain end. After extraction with methylene chloride, MPEO terminated with propylene glycol was obtained by precipitation in cold diethyl ether.

Hydrogels

PEO was dissolved in tetrahydrofuran (THF) containing three drops of dibutyltin dilaurate with an equimolar amount of PTMO or PDMS. Then, hexamethylene diisocyanate (HDI; 2 equiv of PEO) solution in THF was slowly added. The mixture solution was stirred for 1 day at room temperature. It was then precipitated in *n*-hexane and washed with excess amounts of distilled water. The resulting hydrogels, including PEO_{2k}–PTMO, $PEO_{3.4k}$–PTMO, and $PEO_{3.4k}$–PDMS were dried for 2 days at 50°C under vacuum. To obtain hydrogels with PEO grafts ($MPEO_{2k}$–PTMO), MPEO terminated with propylene glycol was also reacted with PTMO in an identical manner.

Characterization

^{1}H-NMR spectroscopy was performed on a Jeol JNM-LA 300 WB FT-NMR, which was operated at 300 MHz with a 6 wt % polymer solution in sulfoxide-d_6 or $CDCl_3$. The molecular weight was determined with gel permeation chromatography (GPC; Waters). A polymer solution (0.2% w/v in THF) was injected into Waters Styragel columns. Molecular weight was determined on the basis of the calibration curve resulting from polystyrene standard samples.

With an aluminum pan containing approximately 10 mg of polymer sample, the thermal properties of the polymers were characterized with a DSC 2100 (TA Instruments). After the samples were quenched with liquid nitrogen, the temperature was vaned from −150 to 150°C at a heating rate of 10°C/min. The samples were purged with anhydrous nitrogen gas during the experiment, and indium was taken as an internal standard for analysis. To evaluate the thermal properties when they were hydrated, the hydrogels, equilibrated at 25°C in distilled water, were sealed tightly in a pan. DSC analysis was then carried out from −50 to 60°C at a heating rate of 2°C/min.

The wide-angle X-ray diffraction (WAXD) pattern was observed with a Rigaku apparatus (Japan) with a Cu Kα source (1.541 Å), in which the samples were mounted on the center of a two-circle X-ray diffractometer (Huber, Germany), and X-rays were generated from an 18-kW rotating anode machine. Consequently, the crystallinity (X_c) of hydrogels was calculated as follows:

$$X_c(\%) = A_c/(A_a + A_c) \quad (1)$$

where A_a is the area under the amorphous hummock and A_c is the area of crystalline peaks except in the hummock region.

Uniaxial stress–strain analysis was performed with an Instron instrument (model 5567) at a crosshead speed of 50 mm/min. At least three separate tensile specimens (0.3 mm in thickness) were prepared with an ASTM D 638M die. The specimens were then tested after being dried in a vacuum for 1 day at room temperature and being hydrated in distilled water for 1 day at room temperature.

To evaluate the swelling behavior of the polymers as a function of immersion time and temperature in PBS (pH = 7.4) solution, the dried polymer films were cut into disk shapes (thickness = 0.3 mm, diameter = 12 mm). After immersion in a PBS (pH = 7.4) solution, the weights of the swollen polymers were measured in the desired periods after the removal of excess surface water by patting the samples with filter paper. The water capacity (W_c) was then calculated by the following equation:

$$W_c = (W_{\text{swollen}} - W_{\text{polymer}})/W_{\text{polymer}} \quad (2)$$

where W_{swollen} is the weight of polymer swollen in PBS and W_{polymer} is the weight of the polymer dried in a vacuum for 1 day at room temperature.

Bacterial adhesion tests

The bacteria used in this study included *S. epidermidis* (ATCC No. 12228) and E. coli (ATCC No. 11775) received from the Korean Collection for Type Cultures. Each of the species, which had been maintained on nutrient agar plate, was cultured for 24 h at 37°C in a nutrient broth (Difco) solution. The bacterial inoculum was then washed twice by centrifuging in PBS (pH = 7.4), resuspended, and adjusted to reach 1×10^8 cells/mL for the bacterial adhesion experiments. The polymer films (12 mm in diameter and 0.1 mm in thickness), which were sterilized by ultraviolet radiation, were exposed to a bacterial suspension (10 mL) and incubated for 2 h at 37°C. After being rinsed with PBS, the resulting films were vertexed and sonicated for 2 min, respectively, with 10 mL of PBS containing 0.1% Tween-80 to detach any bacteria adhering to the

TABLE I
Characteristics of Hydrogels Synthesized in This Study

Polymers[a]	Composition	M_n[b]	M_w[b]	Block ratio[c]
Pellethane	PTMO/MDI/BD	70,908	90,247	—
PEO_{2k}–PTMO	PEO_{2k}/HDI/PTMO	51,566	66,233	0.99
$MPEO_{2k}$–PTMO	$MPEO_{2k}$/HDI/PTMO	37,973	50,834	0.92
$PEO_{3.4k}$–PTMO	$PEO_{3.4k}$/HDI/PTMO	62,436	78,980	1.03
$PEO_{3.4k}$–PDMS	$PEO_{3.4k}$/HDI/PDMS	50,751	62,453	1.03

BD = 1,4-butane diol.
[a] The M_n's of PTMO and PDMS were fixed to 2000 and 1860, respectively.
[b] Estimated by GPC.
[c] Calculated from the integration ratio of the characteristic peaks in PEO and the hydrophobic block, resulting from ^{1}H-NMR.

surfaces, as suggested by Flemming et al.[14] The number of adherent bacteria was quantitatively determined by colony counts and expressed as the number of colony-forming units (CFUs) per square centimeter. The effects of albumin adsorption were assessed by pretreatment of the polymer films with BSA solution (100 μg/mL in PBS) for 2 h at 37°C and a rinse with a PBS solution, followed by bacterial adhesion tests as illustrated previously.

RESULTS AND DISCUSSION

Polymer synthesis

To examine the influence of PEO block length, the hydrophobic block, and the polymer topology of the hydrogels on physical properties and bacterial adhesion, the polymers were prepared by polycondensation reactions between telechelic macromonomers terminated with hydroxyl groups and an aliphatic diisocyanate (HDI). As shown in Table I, the hydrogels synthesized in this study exhibited a high weight-average molecular weight (M_w), ranging from 50,000 to 66,000 and a narrow polydispersity, lower than 1.35. The block ratios, calculated by the integration ratio of the characteristic peak of PEO (3.63 ppm) and those of the hydrophobic segments (3.38 ppm for PTMO and 0 ppm for PDMS) resulting from the ^{1}H-NMR spectra, were close to unity.

Physical properties

The DSC traces of the hydrogels are represented in Figure 2. Typically, the PEO–PTMO hydrogels showed four events, originating from the glass transitions and melting temperatures (T_m's) of the PEO and PTMO blocks. On the other hand, $PEO_{3.4k}$–PDMS exhibited only three transitions due to the absence of PDMS crystalline structure. These were designated as α, β, γ, and δ transitions from high to low temperatures, and the detailed thermal transitions are shown in Table II. The α and β transitions were observed as the T_m's of PEO and PTMO, respectively. The γ transition resulted from the glass transition of PEO, whereas the δ transition originated from the glass transition of the hydrophobic block.

The DSC curves of hydrated polymers during heating showed two endothermic peaks at about 0° and −20°C. The former appeared from the melting of ice (free water region), but the latter was formed by bound water.[15] In contrast to dried polymers, there were no α transitions in the hydrated polymers, suggesting that the crystalline domain was destroyed due to the interaction of the PEO block, responsible for the α transition, with water.[16] Another finding was the slight increase in β transitions in (M) PEO–PTMO hydrogels, which might have been due to the rearrangement of PTMO after hydration.

The α transitions appearing from the dried hydrogels were lower than that of pure PEO (e.g., T_m = 50°C for PEO_{2k}, but T_m = 39°C for PEO_{2k}PTMO, respectively), indicating that the hydrophobic blocks inhibited

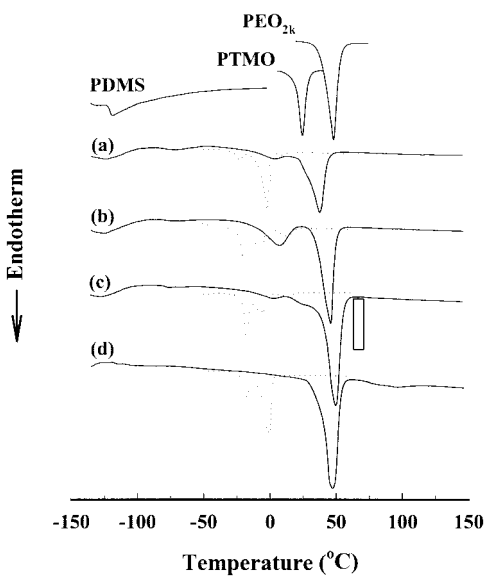

Figure 2 DSC thermograms for (—) dried and (···) hydrated hydrogels as a function of temperature: (a) PEO_{2k}–PTMO, (b) $MPEO_{2k}$–PTMO, (c) $PEO_{3.4k}$–PTMO, and (d) $PEO_{3.4k}$–PDMS.

the formation of PEO crystals. The results also demonstrated that the hydrogels with longer PEO blocks, including $PEO_{3.4k}$–PTMO and $PEO_{3.4k}$–PDMS, showed higher α transitions, possibly caused by the compactly ordered structure. $MPEO_{2k}$–PTMO, showed a higher α transition than PEO_{2k}PTMO, attributed to different polymer topologies, despite their similar composition (see Fig. 1). Also, the restricted mobility of PEO due to the partial mixing with the hydrophobic blocks in PEO/PTMO hydrogels resulted in an increase in γ transitions [e.g., T_g glass-transition temperature = $\sim$ −60°C for PEO_{2k}, but T_g = −38°C for PEO_{2k}–PTMO]: On the contrary, the γ and δ transitions in $PEO_{3.4k}$–PDMS appeared at −56 and −120°C, respectively, which were close to the corresponding homopolymer T_g's. This suggests that the PEO block was strongly phase-separated with PDMS.

The melting peaks of PTMO (β transitions) appearing from the dried (M)PEO–PTMO hydrogels broadened with a range of −25 to 25°C and shifted to lower positions, compared to pure PTMO (Fig. 2). Among the hydrogels studied, the highest β transition was observed in $MPEO_{2k}$–PTMO, which also did not show any detectable glass transition of MPEO. The δ transitions in the (M)PEO–PTMO hydrogels were observed around −80°C, similar to the T_g of the PTMO homopolymer, implying that a distinct amorphous phase of PTMO was formed in the hydrogels.

It has been reported that the crystallization of PEO-based block copolymers is significantly dependent on the hydrophobic blocks.[17–19] For example, when poly(L-lactide) (PLA) was used as a hydrophobic block, the crystallinity of the PEO block approached zero when the molar ratio of PEO to PLA was lower than 40%.[20] In this case the, PLA block was first crystallized on cooling, which might have hindered the mobility of the PEO block. As a consequence, the crystallization of the PEO block was hampered.[21] However, from PEO/poly (ε-caprolactone) (PCL) copolymers, a different phenomenon was reported by Petrova et al.,[22] who found that the copolymer composed of PEO_{2k} and PCL_{2k}, showed a double melting peak, reflecting the presence of two crystalline domains corresponding to the PEO and PCL blocks.

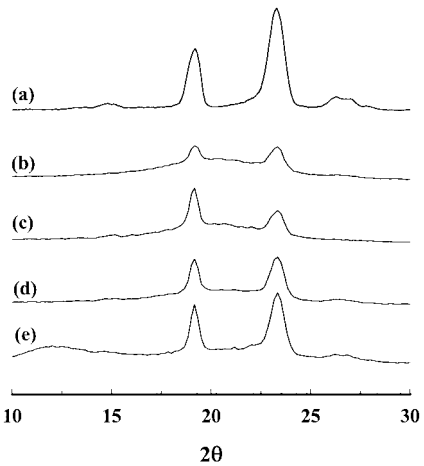

Figure 3 WAXD patterns of hydrogels: (a) PEO_{2k}–PTMO, (b) PEO_{2k}–PTMO, (c) $MPEO_{2k}$–PTMO, (d) $PEO_{3.4k}$–PTMO, and (e) $PEO_{3.4k}$–PDMS.

They also confirmed that after the first-run, the PEO_{2k} crystallized faster than PCL_{2k} during the second run. Similarly, our (M)PEO–PTMO hydrogels exhibited broad and small PTMO endothermic peaks with sharp (M)PEO melting peaks, indicating the higher crystallizability of (M)PEO. Even though the melting peak of PDMS was not observed in $PEO_{3.4k}$–PDMS, its incompatibility with PEO allowed the PEO phase to crystallize readily, as shown in Figure 2.

The WAXD patterns for the hydrogels and PEO homopolymer are shown in Figure 3. PEO_{2k} showed two typical intense peaks at 2θ = 19 and 23, which is consistent with previous reports.[3,22] All of the hydrogels had two main peaks corresponding to PEO, implying that the domain that crystallized in the synthetic polymers dominantly consisted of PEO. The detailed degree of crystallinity for hydrogels was calculated and is listed in Table II.

Compared to PEO_{2k}–PTMO (X_c = 18.17), $MPEO_{2k}$–PTMO (X_c = 28.57) possessed a higher crystallinity. This could be elucidated by the fact that the chain mobility of MPEO in $MPEO_{2k}$–PTMO was enhanced by the free chain end due to lower spatial restriction than PEO in other hydrogels, whose chain ends were

TABLE II
Thermal Transitions and Crystallinity

Hydrogels	Transition temperature (°C)[a]				
	δ	γ	β[b]	α	X_c (%)[c]
PEO_{2k}–PTMO	−80	−38	−10to13(5)	39	18.17
$MPEO_{2k}$–PTMO	−79	—	−25to25(8)	46	28.57
$PEO_{3.4k}$–PTMO	−80	−50	−15to13(4)	49	36.76
$PEO_{3.4k}$–PDMS	−120	−56	—	48	43.50

[a] Obtained from DSC after quenching with liquid nitrogen.
[b] The onset and end temperatures are quoted, and the peak temperature is shown in parentheses.
[c] Estimated from WAXD analysis.

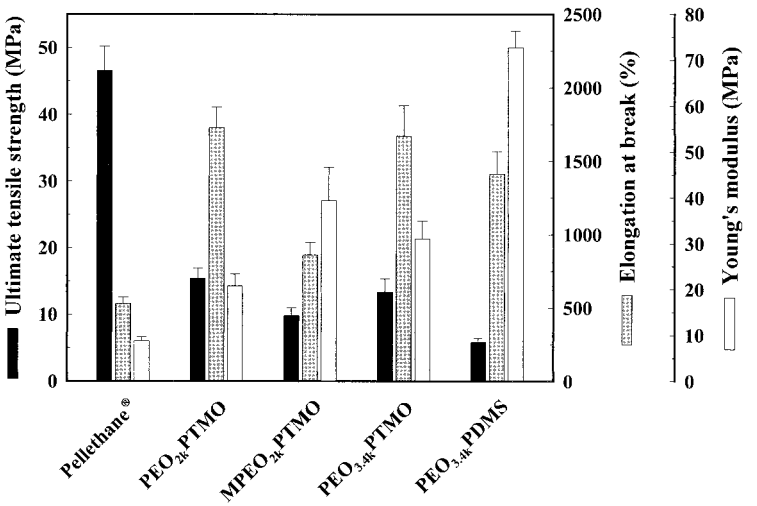

Figure 4 Mechanical properties of hydrogels dried in a vacuum for 1 day (the error bar is for standard deviation, $n = 3$). Films were prepared by the solvent evaporation method with a polymer solution (10 wt % in THF).

both coupled with hydrophobic blocks (Fig. 1). Consequently, this freely mobile grafted chain might have made the formation of an ordered structure easier, resulting in the enhancement of crystallization. When the PEO block length effect, was considered, the increase of that induced higher crystallinity was mainly ascribed to the ordered structure and higher PEO content in the main chain. It was also evident that the hydrogel composed of PDMS as a hydrophobic block ($PEO_{3.4k}$–PDMS, $X_c = 43.50$) exhibited higher crystallinity than that constructed of PTMO ($PEO_{3.4k}$–PTMO, $X_c = 36.76$).

Previous reports demonstrated that PDMS-based copolymers showed extremely phase-separated morphologies due to the low surface energy of PDMS.[23,24] The possibility of phase separation between PEO and PTMO was also suggested by Deslandes et al.[25] Similarly, it could be expected that the constituents of our hydrogels were immiscible to each other. The crystalline formation of PEO obtained from DSC and WAXD studies supported this hypothesis. The highest crystallinity of PEO in $PEO_{3.4k}$–PDMS, close to the crystallinity value of the PEO_{2k} homopolymer ($X_c = 65$), among the hydrogels indicated a strongly segregated morphology resulting from incompatibility between PEO and PDMS, which was in a good agreement with DSC results.

Figure 4 shows the comparative mechanical properties of the hydrogels determined by tensile testing. It was evident from the results that the hydrogels possessed higher Young's moduli; and elongations at break point but lower ultimate tensile strengths compared to Pellethane. This resulted mostly from the crystallinity of PEO and the flexible characteristics of the hydrophobic blocks due to their low glass transitions ($T_g = -80$°C for PTMO and -120°C for PDMS). The Young's moduli of the hydrogels decreased in the order $PEO_{3.4k}$–PDMS > $MPEO_{2k}$–PTMO > $PEO_{3.4k}$–PTMO > PEO_{2k}–PTMO, which was the opposite order of ultimate tensile strength. The crystalline formation and degree of phase separation as described in the DSC and WAXD results might have played an important role in these results. The ultimate tensile strength, elongation at break point, and Young's modulus of all of the hydrogels significantly decreased after hydration (Fig. 5). This might have been due to the disappearance of the PEO crystalline domain, as shown in Figure 2, and the plasticizing effect of adsorbed water.[2] For example, the Young's modulus of the hydrated hydrogels decreased from 11-fold to 44-fold, in which the greater decrease was found in hydrogels with longer PEO blocks and with PTMO as a hydrophobic block; for example; $PEO_{3.4k}$–PDMS exhibited a 40-fold decrease, whereas $PEO_{3.4k}$–PTMO had 44-fold decrease. As shown in Figure 2, the existence of distinct PTMO crystallinity, not soluble in water, might have induced the lowest decrease (11-fold) of Young's modulus in $MPEO_{2k}$–PTMO among the hydrogels. Despite the deterioration of mechanical properties in distilled water, the elongations at break of the hydrogels, except for $PEO_{3.4k}$–PDMS, were still higher than about 700%, which was a larger value compared to that of Pellethane (~530%), due to flexible characteristics.

Swelling behavior

The swellability of the hydrogels as a function of time is shown in Figure 6. Pellethane, used as the hydrophobic control material, showed no significant water uptake for up to 2 h, whereas the hydrogels exhibited time-dependent water uptake profiles, which were typically observed as biphasic, with an initial rapid water uptake followed by a slow equilibrium. The

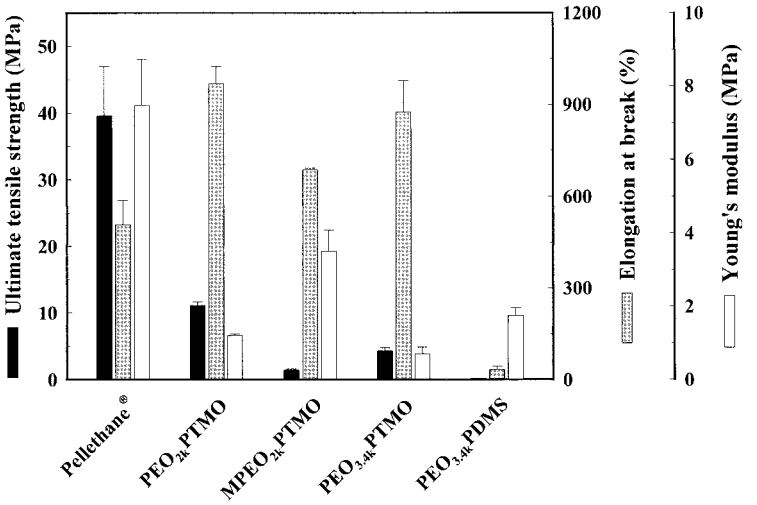

Figure 5 Mechanical properties of hydrogels hydrated in distilled water for 1 day (the error bar is for standard deviation, $n = 3$). Films were prepared by the solvent evaporation method with a polymer solution (10 wt % in THF).

time to reach equilibrium swelling was within 20 min except for $MPEO_{2k}$–PTMO. The slower swelling rate of $MPEO_{2k}$–PTMO among the hydrogels might have been related to the time for the melting of PTMO crystals, as shown in Figure 2. The degree of equilibrium swelling was proportional to the PEO block length. The results also imply that the dominant factor responsible for swelling was the PEO content in our polymer composition because PEO_{2k}–PTMO ($W_c = 1.14$) showed a similar water capacity to $MPEO_{2k}$–PTMO ($W_c = 1.13$). In general, the PEO-based hydrogels, which are chemically crosslinked, take at least 10 h to achieve swelling equilibrium due to the crosslinking agent causing restricted mobility in PEO.[26] In contrast, our hydrogels were physically crosslinked with flexible hydrophobic blocks, which might have allowed the PEO chain to respond rapidly when it contacted water.

Figure 7 shows the effect of temperature on the water capacity for the first and second cycles. The water capacity of the (M)PEO–PTMO hydrogels was higher in the second cycle than in the first cycle, indicating that the swellability was dependant on the thermal cycles. On the contrary, $PEO_{3.4k}$–PDMS did not show significant differences for repeated thermal cycles. These results suggest that the PTMO influenced the swelling behavior. In the first cycle, the water capacity of the PEO–PTMO hydrogels decreased with increasing temperature due to the thermonegativity of the PEO chain. Similarly, previous reports have suggested that the water capacity of hydrogels could decrease with increasing temperature due to weakening

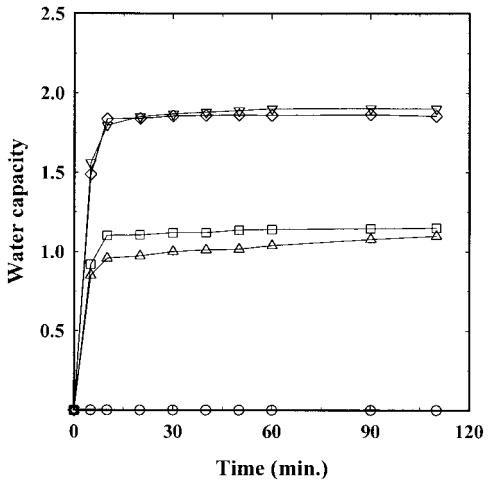

Figure 6 Swelling behavior of hydrogels as a function of time: (○) Pellethane, (□) PEO_{2k}–PTMO, (△) $MPEO_{2k}$–PTMO, (▽) $PEO_{3.4k}$–PTMO, and (◇) $PEO_{3.4k}$–PDMS.

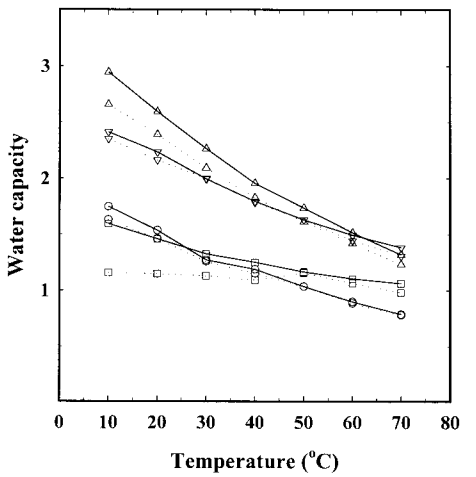

Figure 7 Effect of temperature on the water capacity of the hydrogels for the (···) first and (—) second cycles : (○) PEO_{2k}–PTMO, (□) $MPEO_{2k}$–PTMO, (△) $PEO_{3.4k}$–PTMO, and (▽) $PEO_{3.4k}$–PDMS.

of hydrogen bonding with water and the enhancement of hydrophobic interactions.[26,27] The constant water capacity of $MPEO_{2k}$–PTMO, regardless of increasing temperature, could be elucidated by the increase in hydrophilicity attributed to the disintegration of PTMO crystallinity, which might have been balanced with the decrease in hydrophilicity that arose from PEO. In the second cycle, however, the recrystallization of PTMO in $MPEO_{2k}$–PTMO might not have occurred from the interaction with water, resulting in thermonegative swelling behavior and the higher water uptake in the low-temperature region (< 30°C) compared with the first cycle. This tendency was similar to that of other PEO–PTMO hydrogels.

Bacterial adhesion

Two species of bacteria commonly implicated in biomedical device infections, *S. epidermidis* as a gram-positive bacteria and *E. coli* as a gram-negative bacteria, were adopted to investigate the influence of surface chemistry, polymer topology, and the preadsorption of albumin on bacterial adhesion. Figure 8 shows the bacterial adhesion results for hydrogels that were incubated in PBS (pH = 7.4) only. Previous reports demonstrated that bacteria adheres in higher numbers to hydrophobic surfaces than to hydrophilic surfaces, indicating that the hydrophobic interaction is mainly responsible for bacterial adhesion.[10,11] Similarly, both *S. epidermids* and *E. coli* were found to adhere to the hydrophobic Pellethane surface much greater than to hydrophilic hydrogel surfaces. In addition, all of the hydrogels were more effective in repelling *E. coli* than *S. epidermidis*, in which the differences were approximately a factor of 10; for example, the number of bacteria adhering to PEO_{2k}–PTMO

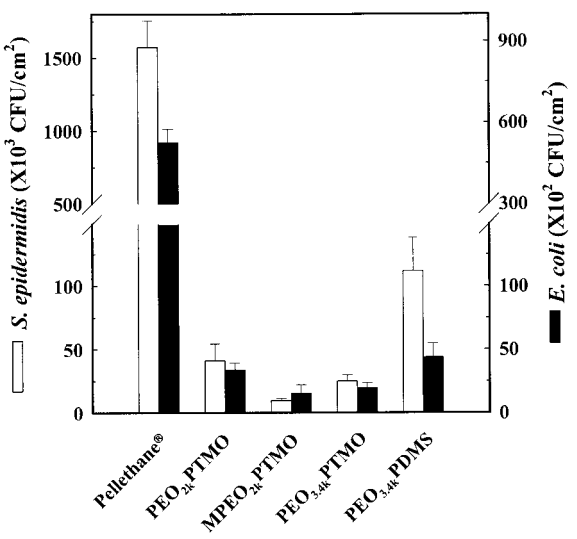

Figure 8 Bacterial adhesion to the hydrogel surfaces (the error bar is for standard deviation, $n = 5$).

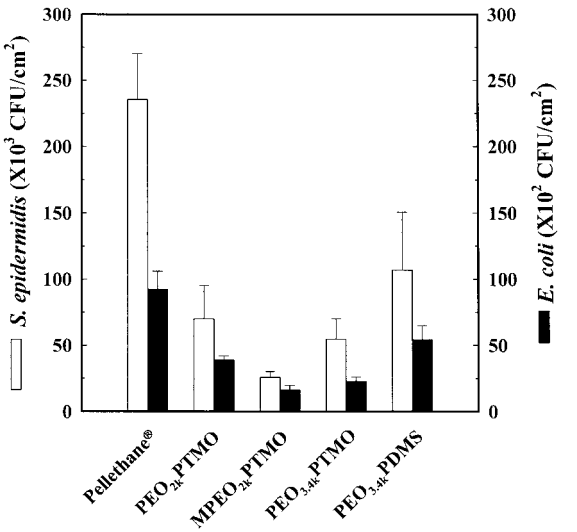

Figure 9 Bacterial adhesion to the hydrogel surfaces preadsorbed with albumin (the error bar is for standard deviation, $n = 5$).

was 41×10^3 CFU/cm^2 for *S. epidermidis* but 34×10^2 CFU/cm^2 for *E. coli*, respectively. Compared to a hydrogel with a short PEO chain (PEO_{2k}–PTMO), that with a longer PEO chain ($PEO_{3.4k}$–PTMO) exhibited a better depression of both *S. epidermidis* and *E. coli* adhesion, which is consistent with other reports.[28,29] Interestingly, the hydrogel with MPEO grafts ($MPEO_{2k}$–PTMO) showed the least adhesion for *S. epidermidis* (10×10^3 CFU/cm^2) and minimized *E. coli* attachment (15×10^2 CFU/cm^2), comparable to $PEO_{3.4k}$–PTMO (19×10^2 CFU/cm^2). This result implies that freely mobile MPEO grafts in $MPEO_{2k}$–PTMO more significantly enhanced the bacterial repellency in an aqueous environment, compared to PEO in the other hydrogels, due to their larger excluded volume, lower interfacial energy, and increased hydrophilicity.[12]

As shown in Figure 8, the hydrogel with PDMS as a hydrophobic block ($PEO_{3.4k}$–PDMS) was more attractive to bacterial adhesion than that with PTMO ($PEO_{3.4k}$–PTMO). PDMS-based polymers have often been limited as biomedical devices due to infection following bacterial adhesion by a hydrophobic interaction between bacteria and polymer surfaces,[30] although they possess good biocompatibility[31] and excellent thermal and oxidative stability, which allows them to be sterilized via versatile routes. In our previous study, $PEO_{3.4k}$–PDMS also exhibited significant protein adsorption, primarily due to the hydrophobic interaction between the PDMS surface exposed in an aqueous environment and plasma protein.[12] Therefore, we suggest that certain amounts of the PDMS domain in the strongly phase-separated hydrogel ($PEO_{3.4k}$–PDMS) were exposed to the outermost layer, which allowed bacteria to be anchored on the polymeric surfaces via hydrophobic interactions.

To assess the effects of adsorbed protein on bacterial adhesion, the polymeric surfaces were preadsorbed with BSA, which is known to create repellent surfaces to cellular adhesion. The results of bacaterial adhesion to the BSA-adsorbed surfaces are shown in Figure 9 for both *S. epidermidis* and *E. coli.* The general trend of bacterial adhesion to albumin-coated surfaces was similar to the results for uncoated surfaces in which the number of adherent bacteria decreased in the order Pellethane > $PEO_{3.4k}$–PDMS > PEO_{2k}–PTMO > $PEO_{3.4k}$–PTMO > $MPEO_{2k}$–PTMO. However, there was a significant decrease in adherent bacteria to the albumin-coated Pellethane surface, compared to a bare surface; for example, the average CFU counts for *S. epidermids* on bare Pellethane were 1573×10^3 CFU/cm^2, whereas 235×10^2 CFU/cm^2 were observed on albumin-coated Pellethane. *E. coli* adhesion also decreased sixfold after coating with albumin. These results are in a good agreement with previous reports.[28,32] For example, Baumgartner and Cooper[33] investigated the influence that protein and cellular components of thombi had in mediating bacterial adhesion on polymeric surfaces. They confirmed that the presence of fibrin or platelets significantly increased *S. aureus* adhesion compared to surfaces preadsorbed with albumin, which was also more than three-fold resistant to bacterial adhesion than were bare surfaces. Although the mechanism of the inhibiting effect of albumin is not clearly understood, albumin may enhance the resistance to bacterial adhesion by changing hydrophobic surfaces into hydrophilic ones.[34,35]

In contrast to Pellethane, there were no significant decreases in bacterial adhesion to hydrogels synthesized in this study after preadsorption of albumin, implying that the adsorbed albumin was not effective in the bacterial repellency of the hydrogels. It is generally believed that hydrophilic polymers such as hydrogels inhibit proteins from adsorbing on the surfaces due to a low interfacial energy.[36] Our results also demonstrated that proteins, including fibrinogen, albumin, and immunoglobulin G, adsorbed much less on the hydrogels than on Pellethane.[12] In addition, the amount of albumin adsorbed on our hydrogels was at least 50% lower than that on Pellethane, and more than 75% of them could be reversibly detached by treatment with a 0.5 wt % sodium dodecyl sulfate solution. Thus, we suggest that the lower amounts of albumin adsorbed on hydrogels neither was enough to cover the entire surface area nor significantly changed the surface properties such as hydrophilicity.

CONCLUSIONS

This investigation explored effects of polymer chemistry and topology on the physical properties and bacterial adhesion of hydrogels. All the hydrogels synthesized in this study showed strongly phase-separated morphologies and unique crystallinities, depending on their polymer compositions and topologies. It was observed from tensile tests that the PEO crystallinity and flexible characteristics of the hydrophobic blocks in the hydrogels resulted in higher Young's moduli and elongations at break, compared to Pellethane. Due to the hydrophilic PEO block, the hydrogels absorbed significant amounts of water and showed thermonegative swelling patterns. The bacterial adhesion results demonstrated that the hydrogels exhibited much lower adhesions of both *S. epidermidis* and *E. coli* than did Pellethane, regardless of albumin treatment. The higher resistance to bacterial adhesion could be achieved by the incorporation of a longer poly(ethylene glycol) chain and the adoption of PTMO as a hydrophobic segment instead of PDMS. In addition, the results suggested that the hydrogel with MPEO grafts (graft copolymer) was more effective in inhibiting the attachment of *S. epidermidis* and *E. coli* than that with PEO (linear copolymer).

References

1. Peppas, N. A. Hydrogels in Medicine and Pharmacy: Properties and Applications; CRC: Boca Raton, FL, 1987; Vol. 3.
2. Anseth, K. S.; Bowman, C. N.; and Brannon-Peppas, L. Biomaterials, 1996, 17, 1657.
3. Cho, C. S.; Jeong, Y. I.; Kim, S. H.; Nah, J. W.; Kubota, M.; Komoto, T. Polymer 2000, 41, 5185.
4. Pezron, E.; Richard, A.; Lafuma, F.; Audebert, R. Macromolecules 1988, 21, 1121.
5. Tanaka, F.; Edward, S. F. Macromolecules 1992, 25, 1516.
6. Gristina, A. G.; Naylor, P. T. In Biomaterials Science: An Introduction to Materials in Medicine; Ratner, B. D.; Hoffman, A. S.; Schoen, F. J.; Lemons, J. E., Eds.; Academic: San Diego, 1996; p 205.
7. Antti-Poika, I.; Josefsson, G.; Konttinen, Y.; Lidgren, L.; Santavirta, S.; Sanzen, L. Acta Orthop Scand 1990, 61, 163.
8. Gristina, A. G.; Costerton, J. W. J Bone Joint Surg Am 1985, 67, 264.
9. An, Y. H.; Friedman, R. J. J Biomed Mater Res 1998, 43, 338.
10. Ong, Y.; Razatos, A.; Georgiou, G.; Sharma, M. M. Langmuir 1999, 15, 2719.
11. Shi, L.; Ardehali, R.; Caldwell, K. D.; Valint, P. Colloids Surf B 2000, 17, 229.
12. Park, J. H.; Bae, Y. H. Biomaterials 2002, 23, 1797.
13. Bergström, K.; Holmberg, K.; Safranj, A.; Hoffman, A. S.; Edgell, M. J.; Kozlowski, A.; Hovanes, A.; Harris, J. M. J Biomed Mater Res 1992, 26, 779.
14. Flemming, R. G.; Capelli, C. C.; Cooper, S. L.; Proctor, R. A. Biomaterials 2000, 21, 273.
15. Antonsen, K. P.; Hoffman, A. S. In Poly(ethylene glycol) Chemistry and Biological Applications; Harris, J. M.; Zalipsky, S., Eds.; Plenum: New York, 1992; p 15.
16. Graham, N. B. In Poly(ethylene glycol) Chemistry and Biological Applications; Harris; J. M.; Zalipsky, S., Eds.; Plenum: New York, 1992; p 263.
17. Kong, X.; Yang, X.; Zhou, E.; Ma, D. Eur Polym J 2000, 36, 1085.
18. Lucke, A.; Teβmar, J.; Schnell, E.; Schmeer, G.; Göpferich, A. Biomaterials 2000, 21, 2361.

19. Chang, Y.; Kwon, Y. C.; Lee, S. C.; Kim, C. Macromolecules 2000, 33, 4496.
20. Youxin, L.; Kissel, T. J. J Controlled Rel case 1993, 27, 247.
21. Huh, K. M.; Bae, Y. H. Polymer , 40, 6147.
22. Petrova, T.; Manolova, N.; Rashkov, I.; Ki, S.; Vert, M. Polym Int 1998, 45, 419.
23. Chu, J. H.; Rangarajan, P.; Asams, J. L.; Register, R. A. Polymer, 1995, 36, 1569.
24. Pasquale, G. D.; Rosa, A. L.; Mamo, R. A. Macromol Rapid Commun 1997, 18, 267.
25. Deslandes, Y.; Pleizier, G.; Alexander, D.; Santerre, P. Polymer 1998, 39, 2361.
26. Iza, M.; Stoianovici, G.; Viora, L., Grossiord, J. L.; Couarraze, G. J Controlled Release 1998, 52, 41.
27. Yoshida, R.; Uchida, K.; Kaneko, Y.; Sakai, K.; Kikuchi, A.; Sakurai, Y.; Okano, T. Nature 1995, 374, 240.
28. Paulsson, M.; Kober, M.; Freij-Larsson, C.; Stollenwerk, M.; Wesslen, B.; Ljungh, Å. Biomaterials 1993, 14, 845.
29. Park, K. D.; Kim, Y. S.; Han, D. K.; Kim, Y. H.; Lee, E. H. B.; Suh, H.; Choi, K. S. Biomaterials 1998, 19, 851.
30. Gottenbos, B.; van der Mei, H. C.; Busscher, H. J. J Biomed Mater Res 2000, 50, 208.
31. Lim, F.; Yang, C. Z.; Cooper, S. L. Biomaterials 1994, 15, 408.
32. Baumgartner, J. N.; Cooper, S. L. J Biomed Mater Res 1998, 40, 660.
33. Baumgartner, J. N.; Cooper, S. L. ASAIO J 1996, 42, M476.
34. Fletcher, M.; Marshall, K. C. Appl Environ Microbiol 1982, 44, 184.
35. Pringle, J. H.; Fletcher, M. Appl Environ Microbiol 1986, 51, 1321.
36. Slack, S. M.; Posso, S. E.; Horbett, T. A. J Biomater Sci Polym Ed 1991, 3, 49.